Flow and heat transfer of a micropolar fluid sandwiched between viscous fluid layers

J.C. Umavathi, J. Prathap Kumar, and A.J. Chamkha

Abstract: In the present analysis, a two-fluid model for blood flow through a horizontal channel is studied. The model essentially consists of a core region assumed to be a micropolar fluid and two viscous (Newtonian) fluid regions. Using the boundary and interface conditions proposed by Ariman et al. (*J. Appl. Mech. ASME,* **41**, 1 (1974)), analytical expressions for velocity, microrotation velocity, and temperature are obtained. The solutions are also evaluated numerically and shown graphically for various governing parameters such as the material parameter, viscosity ratio, conductivity ratio, Eckert and Prandtl numbers on velocity, microrotation velocity, and temperature profiles. In addition, results for the rate of heat transfer, mass flow rate, and skin friction for different values of the physical parameters are presented in tabular form. It is found that effect of the material parameter is to suppress the flow and the viscosity ratio promotes the flow. It is also interesting to note that the material parameter and viscosity ratio affect the position of the point of flow separation for which the flow nature is reversed. Also, considering the solvent viscosity for air, water, and glycerin, the cell rotation on the flow has been tabulated for 0%, 20%, and 40% concentration.

PACS Nos.: 44.15+a, 44.35.+c

Résumé : Nous analysons ici un modèle à deux fluides de l'écoulement sanguin dans un canal horizontal. Le modèle est constitué d'une région noyau constituée d'un fluide micropolaire et de deux régions de fluide visqueux (Newtonien). Utilisant les conditions aux surfaces et aux interfaces d'Ariman et al. (*J. Appl. Mech. ASME,* **41**, 1 (1974)), nous avons obtenu des expressions analytiques pour la vitesse, la vitesse de microrotation et la température. Les solutions ont également été obtenues numériquement et nous les affichons graphiquement pour différentes valeurs des paramètres de contrôle comme le paramètre matériel, le rapport de viscosité, le rapport de conductivité, les nombres de Eckert et de Prandtl sur la vitesse, la vitesse de microrotation et les profiles de température. Nous présentons aussi des tables de résultats sur le taux d'écoulement en masse et la friction de surface pour différentes valeurs des paramètres physiques. Nous observons que l'effet du paramètre matériel est de supprimer l'écoulement, alors que le rapport de viscosité l'augmente. Il est intéressant de noter que le paramètre matériel et le rapport de viscosité affectent la position du point de séparation d'écoulement pour lequel la nature de l'écoulement s'inverse. De plus, considérant la viscosité du solvant pour l'air, l'eau et la glicérine, nous présentons des tables de résultats pour la rotation de la cellule pour des concentration de 0 %, 20 % et 40 %.

[Traduit par la Rédaction]

1. Introduction

The theory of micropolar fluids has received much attention in the last several years because the traditional Newtonian fluids cannot precisely describe the characteristics of fluid flow for a fluid with suspended particles. Physically micropolar fluids may be described as the non-Newtonian fluids consisting of dumb-bell molecules or short rigid cylindrical elements, polymer fluids, fluid suspensions, animal blood, etc. The presence of dust or smoke, particularly in a gas, may also be modeled using micropolar fluid dynamics. The theory of micropolar fluids, first proposed by Eringen [1, 2] is capable of describing such fluids. In this theory the local effects arising from the microstructure and the intrinsic motion of the fluid elements are taken into account. This is a kind of continuum mechanics, and many classical flows are being re-examined to determine the effects of fluid microstructure [3–5]. This theory also fully explains the inertial characteristics of the substructure particles that are also allowed to undergo rotation and deformations. Early studies and application of micropolar fluid mechanics can be found in the review article by Peddieson and McNitt [6], and Ariman et al. [7] and in the recent books by Łukaszewicz [8] and Eringen [9]. Studies of these fluids have received considerable attention due to their application in a number of processes that occur in industry. Such applications include the extrusion of polymer fluids, solidification of liquid crystals, cooling of a metallic plate in a bath, animal bloods, exotic lubricants, and colloidal and suspension solutions, for example, for which the classical Navier–Stokes theory is inadequate.

Since the early investigation of Bayliss [10], several theoretical and experimental attempts have been made to study blood-flow characteristics [11–13]. All these studies have been carried out on the proposition that blood behaves like a Newtonian fluid. However, it has now been accepted that blood behaves like a non-Newtonian fluid under certain flow conditions, in particular at low shear rate. The recent experimental investigations [14–16] on blood flow indicate that under certain flow conditions,

Received 12 October 2007. Accepted 14 February 2008. Published on the NRC Research Press Web site at http://cjp.nrc.ca/ on 8 August 2008.

J.C. Umavathi and J. Prathap Kumar. Department of Mathematics, Gulbarga University, Gulbarga 585 106, Karnataka, India.
A.J. Chamkha.[1] Manufacturing Engineering Department, The Public Authority for Applied Education and Training, Shuweikh, 70654, Kuwait.

[1] Corresponding author (e-mail: chamkha@paaet.edu.kw).

 doi: 10.1139/P08-022

Fig. 1. Physical configuration.

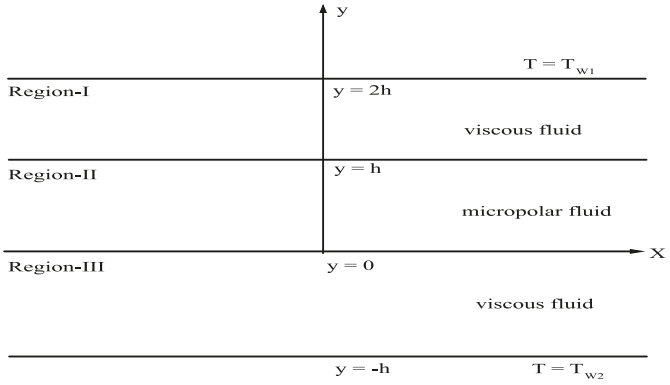

blood flow has deviations from Newtonian flow behavior. It was observed that slurries in general and animal blood in particular show strong deviation from Newtonian behavior.

In recent times, the problem of fluid flow through channels has received considerable attention due to its application to the cardiovascular system [17] treating blood as a micropolar fluid. Ariman et al. [18] examined the blood flow in a rigid circular tube and concluded that the micropolar fluid model is a better model for blood because it accounts for the microrotation of blood suspensions and this analysis is further confirmed by the experimental results of Bugliarello and Sevilla [14]. Bugliarello and Sevilla [14], and Haynes [19] assumed that either both layers, i.e., the peripheral layer of plasma and the core region, are Newtonian fluids or both layers are non-Newtonian fluids. This seems to be improper because it has been shown experimentally [14, 16] that plasma is a Newtonian fluid and the core behaves like a non-Newtonian fluid. Looking at the good agreement obtained by Ariman et al. [18] for velocity profiles and the experimental evidence in support of a two-fluid model and keeping in view the physiological and clinical importance the present problem is posed with the peripheral layer of a Newtonian fluid and the core of a micropolar fluid [18], in a horizontal channel by taking the viscosity of the core fluid as the shear viscosity of blood.

2. Mathematical formulation

Let us consider a steady, laminar, and fully developed flow of blood through a rigid horizontal channel. Based on the experimental results of Bugliarello and Sevilla [14], it is assumed that the blood flow is represented by a two-fluid model with core of micropolar fluid [18] and peripheral layer of plasma as a Newtonian fluid of thickness h as shown in Fig. 1. Under these assumptions the equations for steady, one-dimensional velocity, microrotation velocity, and temperature can be written as

$$(\mu+\kappa)\frac{\mathrm{d}^2u_2}{\mathrm{d}y^2}+\kappa\frac{\mathrm{d}N}{\mathrm{d}y}-\frac{\partial p}{\partial x}=0 \tag{1a}$$

$$\gamma\frac{\mathrm{d}^2N}{\mathrm{d}y^2}-2\kappa N-\kappa\frac{\mathrm{d}u_2}{\mathrm{d}y}=0 \tag{1b}$$

$$k\frac{\mathrm{d}^2T_2}{\mathrm{d}y^2}+\mu\left(\frac{\mathrm{d}u_2}{\mathrm{d}y}\right)^2=0 \tag{1c}$$

for $0 \le y \le 2h$,

$$\mu_1\frac{\mathrm{d}^2u_1}{\mathrm{d}y^2}-\frac{\partial p}{\partial x}=0 \tag{2a}$$

$$k_1\frac{\mathrm{d}^2T_1}{\mathrm{d}^2y}+\mu_1\left(\frac{\mathrm{d}u_1}{\mathrm{d}y}\right)^2=0 \tag{2b}$$

for $-h \le y \le 0$, and

$$\mu_1\frac{\mathrm{d}^2u_3}{\mathrm{d}y^2}-\frac{\partial p}{\partial y}=0 \tag{3a}$$

$$k_1\frac{\mathrm{d}^2T_3}{\mathrm{d}y^2}+\mu_1\left(\frac{\mathrm{d}u_3}{\mathrm{d}y}\right)^2=0 \tag{3b}$$

for $h \le y \le 2h$.

Here, u_i $(i = 1, 2, 3)$ is the x-component of the fluid velocity in the three regions, T_i $(i = 1, 2, 3)$ is the fluid temperature in the three regions, N is the component of microrotation, κ is the vortex viscosity, μ_1 is the viscosity of the clear fluid, μ is the viscosity of the micropolar fluid, k_1 is the thermal conductivity of the fluids in regions I and III, k_2 is the thermal conductivity of the fluid in the region II, γ is the spin-gradient viscosity, and $\partial p/\partial z$ is the constant pressure gradient. Further, it is assumed that γ has the following form as proposed n refs. 20–22

$$\gamma=\left(\mu+\frac{\kappa}{2}\right)j=\mu\left(1+\frac{K}{2}\right)j \tag{4}$$

where $K = \kappa/\mu$ is called the material parameter and j is the microinertia density.

To solve the above system, (1)–(3), eight boundary conditions are required for the velocity and six boundary conditions for the temperature. The first two boundary conditions are obtained from the fact that there is no slip near the wall. The next two conditions are obtained by assuming the continuity of velocity and the last four conditions are obtained from the equality of stresses at the interface and constant cell rotational velocity at the interface as proposed by Ariman et al. [18]. Thus, the appropriate boundary and interface conditions on the velocity in mathematical form are

$$u_1(2h)=0,\quad u_3(-h)=0,\quad u_1(h)=u_2(h),\quad u_2(0)=u_3(0)$$

$$\mu_1\frac{\mathrm{d}u_1}{\mathrm{d}y}=(\mu+\kappa)\frac{\mathrm{d}u_2}{\mathrm{d}y}+\kappa N \quad \text{at } y=h$$

$$(\mu+\kappa)\frac{\mathrm{d}u_2}{\mathrm{d}y}+\kappa N=\mu_1\frac{\mathrm{d}u_3}{\mathrm{d}y} \quad \text{at } y=0$$

$$\frac{\mathrm{d}N}{\mathrm{d}y}=0 \quad \text{at } y=0$$

$$\frac{\mathrm{d}N}{\mathrm{d}y}=0 \quad \text{at } y=h \tag{5}$$

The six boundaries and interface conditions on the temperature are as follows: the upper plate is held at a temperature T_{w1} and the lower plate is held at a temperature T_{w2} with $T_{w1} > T_{w2}$. The other four conditions are the continuity of temperature and

Fig. 2. Effects of the material parameter K on the velocity profiles.

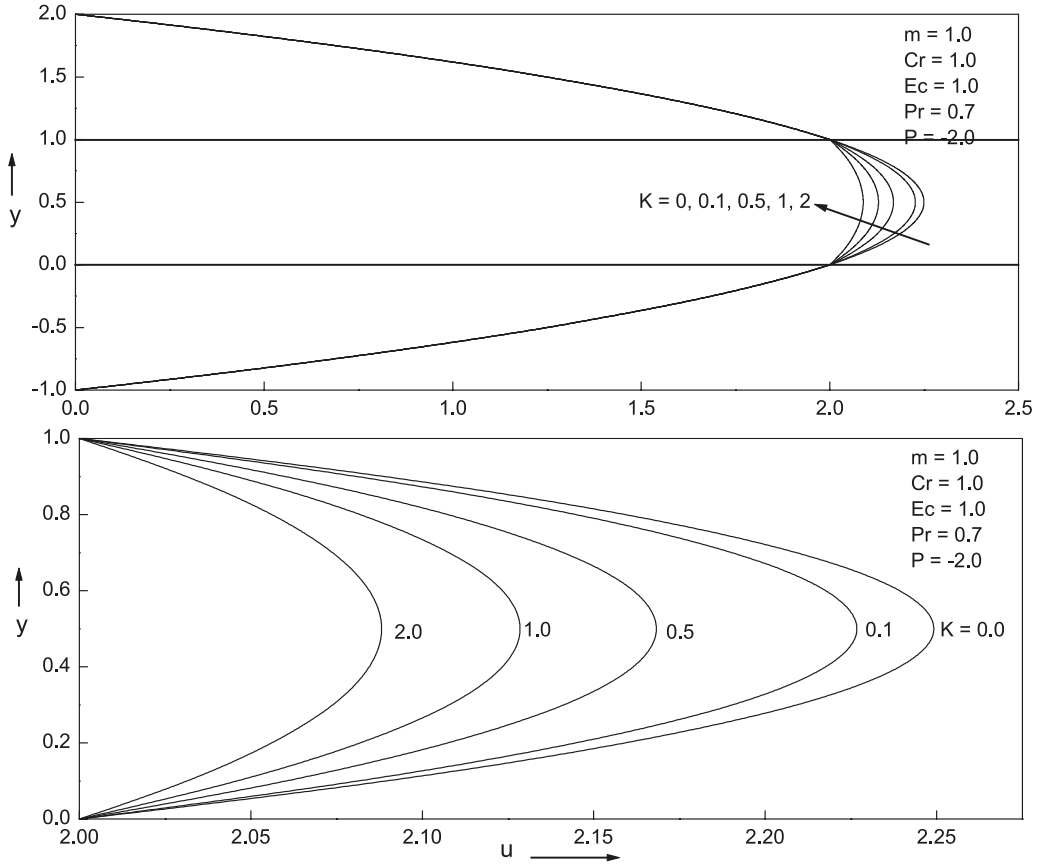

heat flux at the two interfaces.

$$T_1(2h) = T_{w1}, \quad T_3(-h) = T_{w2}, \quad T_1(h) = T_2(h), \quad T_2(0) = T_3(0)$$

$$k_1 \frac{dT_1}{dy} = k_2 \frac{dT_2}{dy} \quad \text{at } y = h$$

$$k_2 \frac{dT_2}{dy} = k_1 \frac{dT_3}{dy} \quad \text{at } y = 0 \tag{6}$$

Equations (1) to (3) and (5) are now made dimensionless by using the following quantities:

$$u_1^* = \frac{u_1}{\bar{u}_1}, \quad y^* = \frac{y}{h}, \quad \theta_i = \frac{T_1 - T_{w2}}{T_{w1} - T_{w2}}, \quad N^* = \frac{h}{\bar{u}_1} N \tag{7}$$

where $\bar{u}_1$ is the average velocity and we take $j = h^2$ as the reference length. These new variables yield, after dropping the asterisk, the following equations in the three regions:

Region – I

$$\frac{d^2 u_1}{dy} = P \tag{8a}$$

$$\frac{d^2 \theta_1}{dy^2} + Ec \ \mathrm{Pr} \left(\frac{du_1}{dy}\right)^2 = 0 \tag{8b}$$

Region – II

$$(1 + K) \frac{d^2 u_2}{dy^2} + K \frac{dN}{dy} - mP = 0 \tag{9a}$$

$$\left(1 + \frac{K}{2}\right) \frac{d^2 N}{dy^2} - 2KN - K \frac{du_2}{dy} = 0 \tag{9b}$$

$$\frac{d^2 \theta_2}{dy^2} + \frac{Ec \ Pr \ Cr}{m} \left(\frac{du_2}{dy}\right)^2 = 0 \tag{9c}$$

Region –III

$$\frac{d^2 u_3}{dy^2} = P \tag{10a}$$

$$\frac{d^2 \theta_3}{dy^2} + Ec \ Pr \left(\frac{du_3}{dy}\right)^2 = 0 \tag{10b}$$

where

$$m = \frac{\mu_1}{\mu_2}, \quad Cr = \frac{k_1}{k_2}, \quad P = \frac{h^2}{\mu_1 \bar{u}_1} \frac{\partial p}{\partial x}, \quad Ec = \frac{\bar{u}_1^2}{Cp\,(T_{w1} - T_{w2})}, \quad Pr = \frac{\mu_1 Cp}{k_1} \tag{11}$$

with Ec being the Eckert number and Pr the Prandtl number, respectively. The nondimensional form of the velocity, temper-

Fig. 3. Effects of the viscosity ratio m on the velocity profiles.

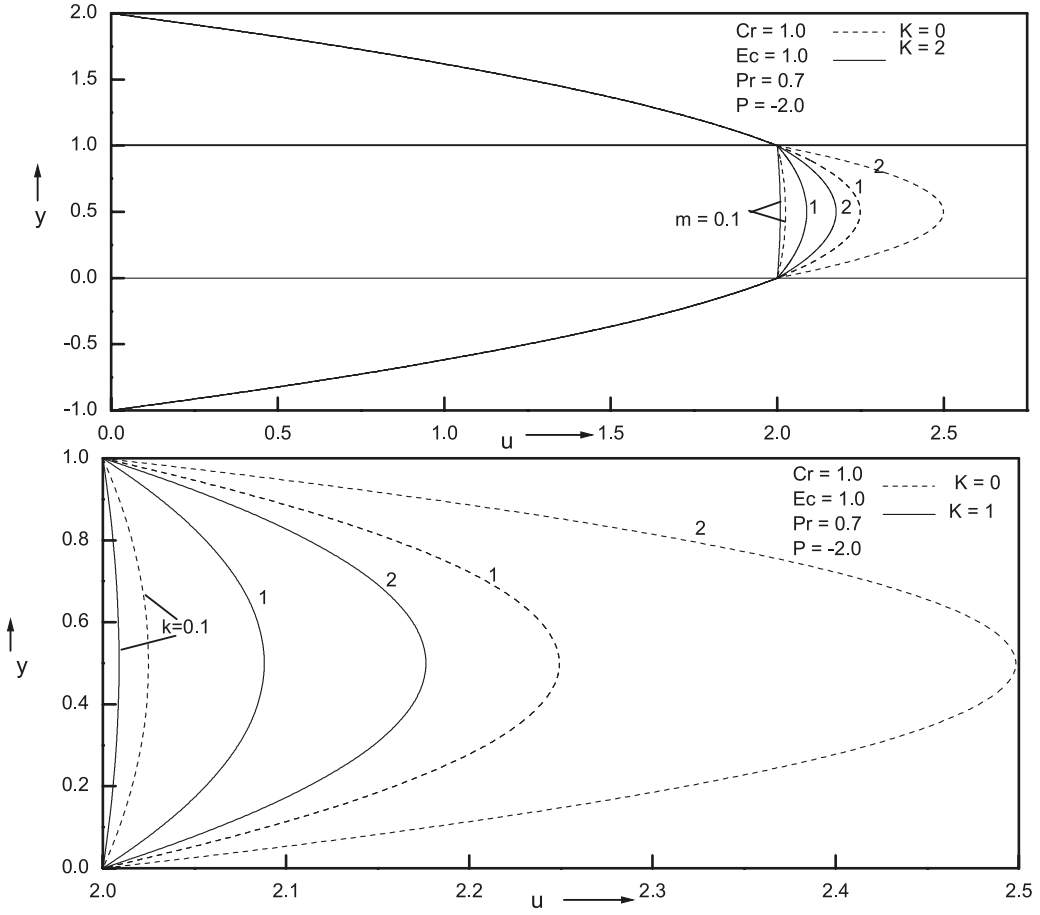

ature boundary, and interface conditions becomes

$$u_1(2) = 0, \quad u_1(1) = u_2(1), \quad u_2(0) = u_3(0), \quad u_3(-1) = 0$$
$$\frac{du_1}{dy} = \left(\frac{1+K}{m}\right)\frac{du_2}{dy} + \frac{K}{m}N \quad \text{at } y = 1$$
$$\left(\frac{1+K}{m}\right)\frac{du_2}{dy} + \frac{K}{m}N = \frac{du_3}{dy} \quad \text{at } y = 0$$
$$\frac{dN}{dy} = 0 \quad \text{at } y = 0$$
$$\frac{dN}{dy} = 0 \quad \text{at } y = 1 \tag{12}$$

$$\theta_1(2) = 1, \quad \theta_1(1) = \theta_2(1), \quad \theta_2(0) = \theta_3(0), \quad \theta_3(-1) = 0$$
$$\frac{d\theta_1}{dy} = \frac{1}{Cr}\frac{d\theta_2}{dy} \quad \text{at } y = 1$$
$$\frac{d\theta_2}{dy} = Cr\frac{d\theta_3}{dy} \quad \text{at } y = 0 \tag{13}$$

3. Closed-form solutions

The expressions for the non-dimensional velocities u_i ($i = 1, 2, 3$), the microrotation velocity N, and the temperatures θ_i ($i = 1, 2, 3$) obtained as the solutions of (8)–(10) with boundary and interface conditions (12) and (13) are:

Region – I

$$u_1 = \frac{P}{2}y^2 + d_1 y + d_2$$
$$\theta_1 = l_4 y^4 + l_5 y^3 + l_6 y^2 + e_1 y + e_2 \tag{14}$$

Region – II

$$u_2 = l_1 \cosh ay + l_2 \sinh ay + l_3 y^2 + d_5 y + d_6$$
$$N = d_3 \cosh ay + d_4 \sinh ay - \frac{mp}{K+2}y - \frac{(K+1)}{(K+2)}A$$
$$\theta_2 = l_7 \cosh 2ay + l_8 \sinh 2ay + l_9 y \cosh ay + l_{10} y \sinh ay + l_{11} \cosh ay + l_{12} \sinh ay + l_{13} y^4 + l_{14} y^3 + l_{15} y^2 + e_3 y + e_4 \tag{15}$$

Region – III

$$u_3 = \frac{P}{2}y^2 + d_7 y + d_8$$
$$\theta_3 = l_{16} y^4 + l_{17} y^3 + l_{18} y^2 + e_5 y + e_6 \tag{16}$$

where the expressions of the constant are not given due to want of space. Further, we shall consider some particular cases of the problem under consideration.

Fig. 4. Effects of the material parameter K on the temperature profile.

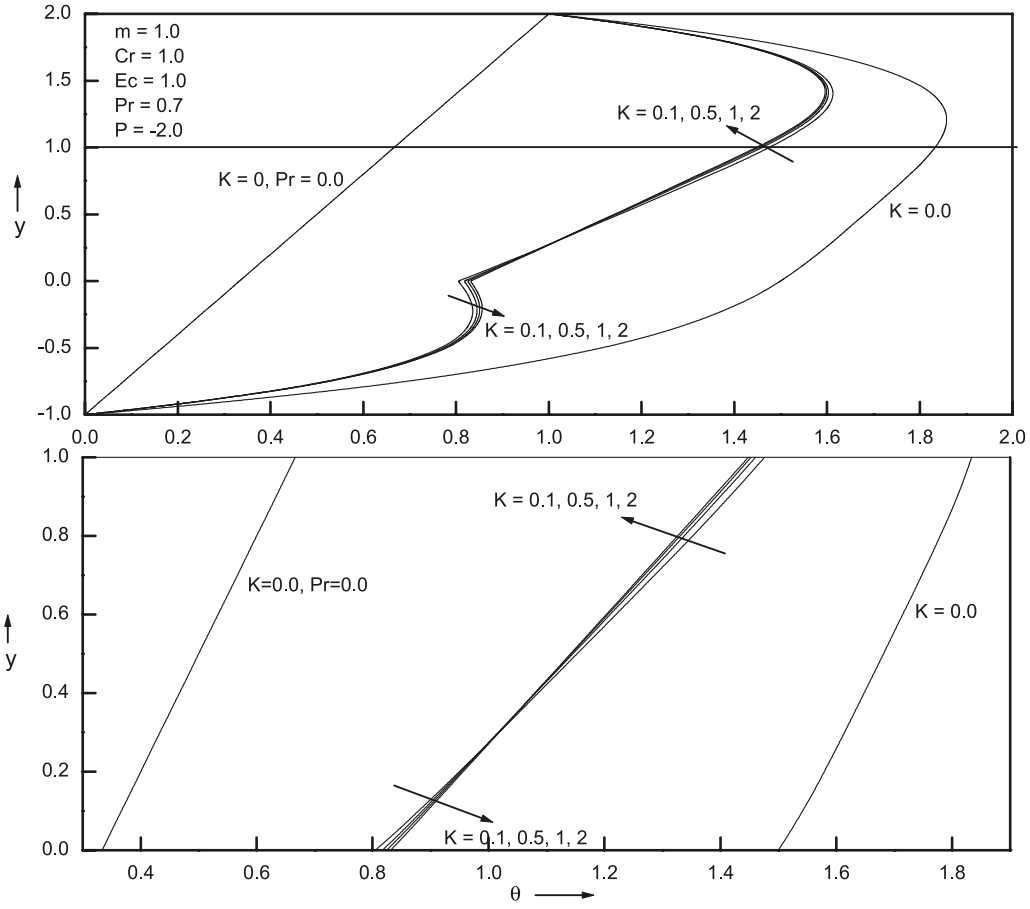

Case – I

For a Newtonian fluid ($K = 0$), the solutions of (8)–(10) are

$$u_1 = \frac{P}{2}y^2 + f_1 y + f_2$$
$$\theta_1 = a_1 y^4 + a_2 y^3 + a_3 y^2 + g_1 y + g_2$$
$$u_2 = \frac{mP}{2}y^2 + f_3 y + f_4$$
$$\theta_2 = a_4 y^4 + a_5 y^3 + a_6 y^2 + g_3 y + g_4$$
$$u_3 = \frac{P}{2}y^2 + f_5 y + f_6$$
$$\theta_3 = a_7 y^4 + a_8 y^3 + a_9 y^2 + g_5 y + g_6 \qquad (17)$$

Case – II

For a Newtonian fluid ($K = 0$) and in the absence of viscous dissipation ($Ec = 0$) the solutions of (8)–(10) reduce to

$$\theta_i = \frac{y+1}{3} \qquad (18)$$

($i = 1, 2, 3$). Since the velocity is independent of the temperature, solutions remain the same as in the above case.

Case – III

The solutions of (8)–(10) in the absence of viscous dissipation ($Ec = 0$) and $K = 0$ for one fluid (i.e., $\mu = \mu_1$) are

$$u_i = \frac{P}{2}y^2 - \frac{P}{2}y - 3P \qquad (19)$$

($i = 1, 2, 3$). The solution for the temperature remains the same as in Case–II.

4. Determination of viscosity of the micropolar fluid

Because of the importance of viscosity [23], from a physiological as well as an engineering point of view, the shear viscosity μ of the micropolar fluid can be determined by knowing the stresses τ_i at any point

$$\tau_i = \mu_i \frac{\mathrm{d}u_i}{\mathrm{d}y} \qquad (20)$$

($i = 1, 3$). Using the solution of (3a), the viscosity of the micropolar fluid μ can be obtained from

$$\tau_3 = -P\,h + \mu_1\,t\,d_7 \qquad (21)$$

This expression is the expression of the effective viscosity in the cylindrical polar coordinates of Chaturani and Upadhya [24] and when $h = 1$ and $\mu = \mu_1$, the above expression reduces to the expression of Ariman et al. [18] in cylindrical polar coordinates for $\kappa = \mu\,K$.

5. Determination of heat transfer, skin friction, and mass flow rate

Apart from the velocity and temperature distribution in the channel, it is important to determine the physical quantities such

Fig. 5. Effect of the viscosity ratio m on temperature profiles.

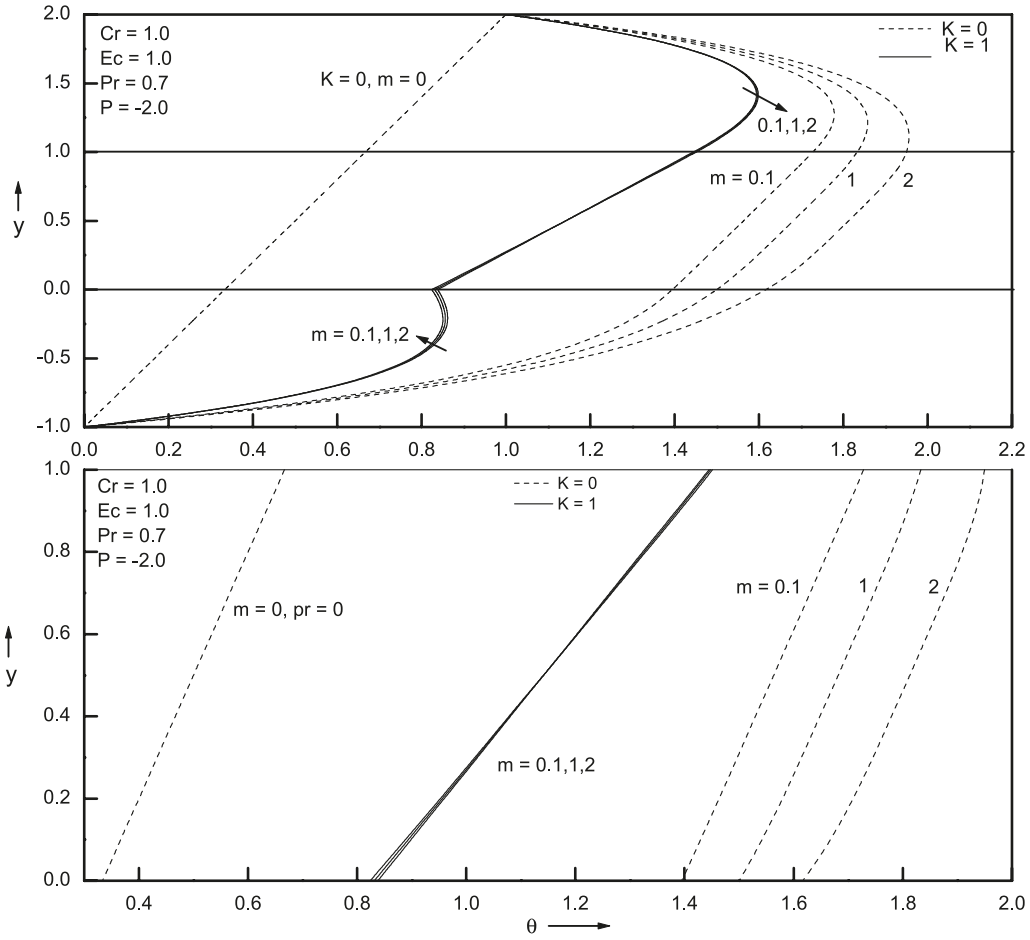

as the rate of heat transfer, the skin friction, and the mass flow rate.

(*i*)**Rate of heat transfer** Knowing the temperature distribution one can determine the non-dimensional rate of heat transfer q from the channel walls to the fluid by the expression

$$q = \left(\frac{\mathrm{d}\theta}{\mathrm{d}y}\right)_{y=-1,2} \tag{22}$$

The rates of heat transfer at the top and bottom walls q_{T} and q_{B} are given in non-dimensional form by

$$q_{\mathrm{T}} = 196l_4 + 48l_5 + 4l_6 + e_1$$
$$q_{\mathrm{B}} = -4l_{16} + 3l_{17} - 2l_{18} + e_5 \tag{23}$$

(*ii*)**Skin friction** The skin frictions at the top and bottom plates τ_{T} and τ_{B} are given in non-dimensional form by

$$\tau = \left(\frac{\mathrm{d}u}{\mathrm{d}y}\right)_{y=-1,2} \tag{24}$$

or

$$\tau_{\mathrm{T}} = 2P + d_1, \qquad \tau_{\mathrm{B}} = -P + d_7 \tag{25}$$

(*iii*)**Mass flow rate** Keeping in view the physical importance, the mass flow rate through the channel is computed and is given by

$$\int_{-1}^{2} u\,\mathrm{d}y = \frac{l_1}{a}\sinh a + \frac{l_2}{a}\cosh a + \frac{l_3}{3} + \frac{d_5}{2} + d_6 - \frac{l_2}{a} + \frac{4P}{3} + \frac{3d_1}{2} + d_2 - \frac{d_7}{2} + d_8 \tag{26}$$

6. Results and discussion

An analytical solution for the problem of flow and heat transfer of a micropolar fluid sandwiched between fluid layers is analyzed. The analytical solutions for (8)–(10) are evaluated numerically for different values of the governing parameters and the results are presented graphically in Figs. 2–12.

The effect of material parameter K on the velocity profiles is shown in Fig. 2. It can be seen that as K increases, the velocity decreases. It is also interesting to note that as K increases the velocity profiles in region-II go on changing from blunt to straight. Figure 3 displays the effect of the viscosity ratio m on the velocity profiles in the presence and absence of the material parameter K. We notice that as m increases the velocity also increases, but the magnitude of promotion is large for $K = 0$

Fig. 6. Effects of the Prandtl number *Pr* on the temperature profiles.

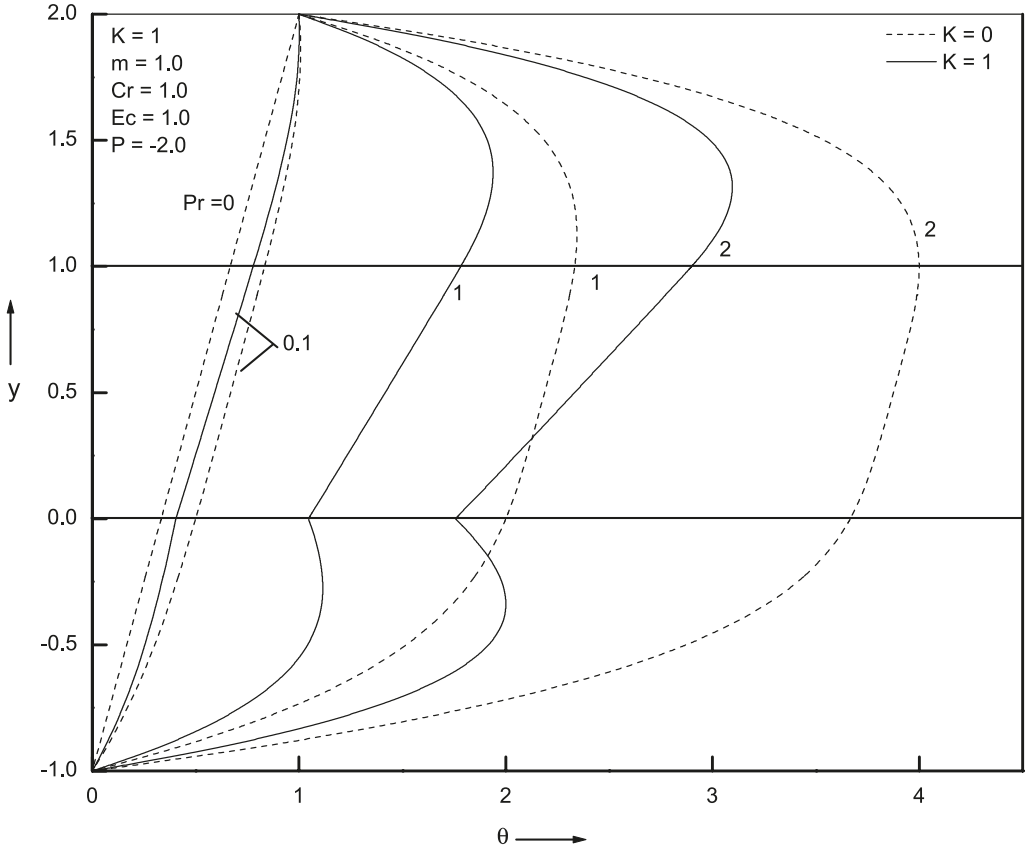

Fig. 7. Effects of the Eckert number *Ec* on the temperature profiles.

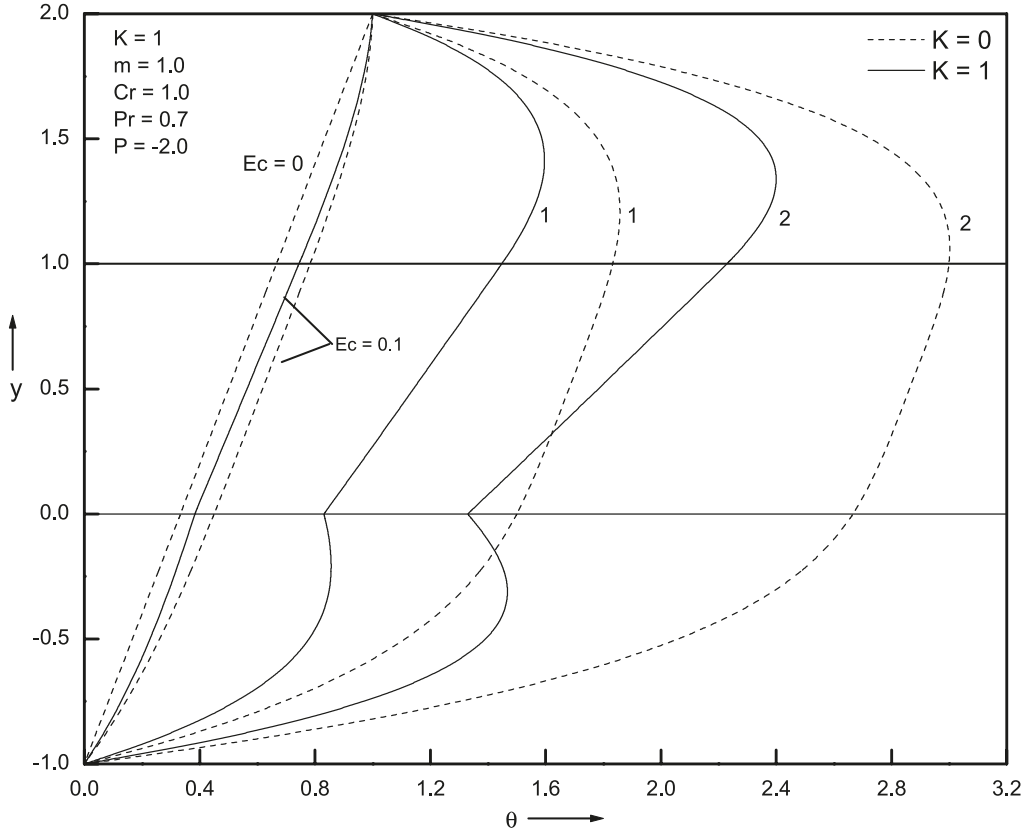

Fig. 8. Effect of the conductivity ratio Cr on the temperature profiles.

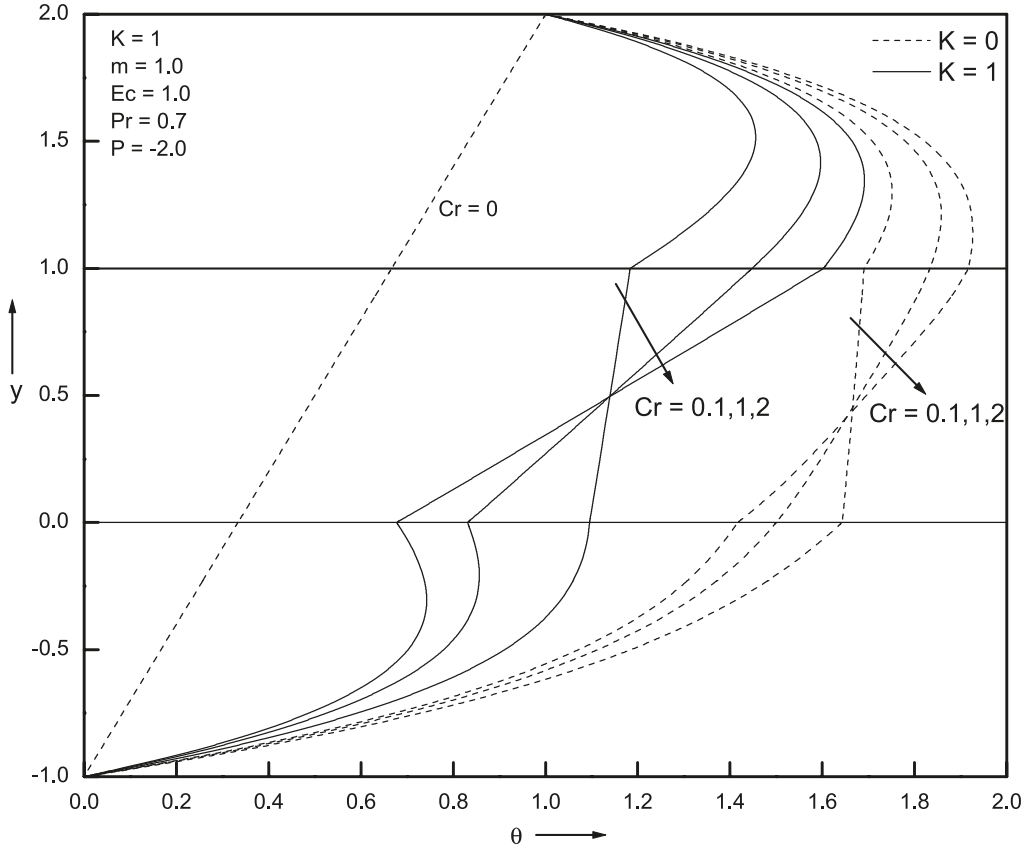

Fig. 9. Effects of the material parameter k on the microrotation velocity profiles N.

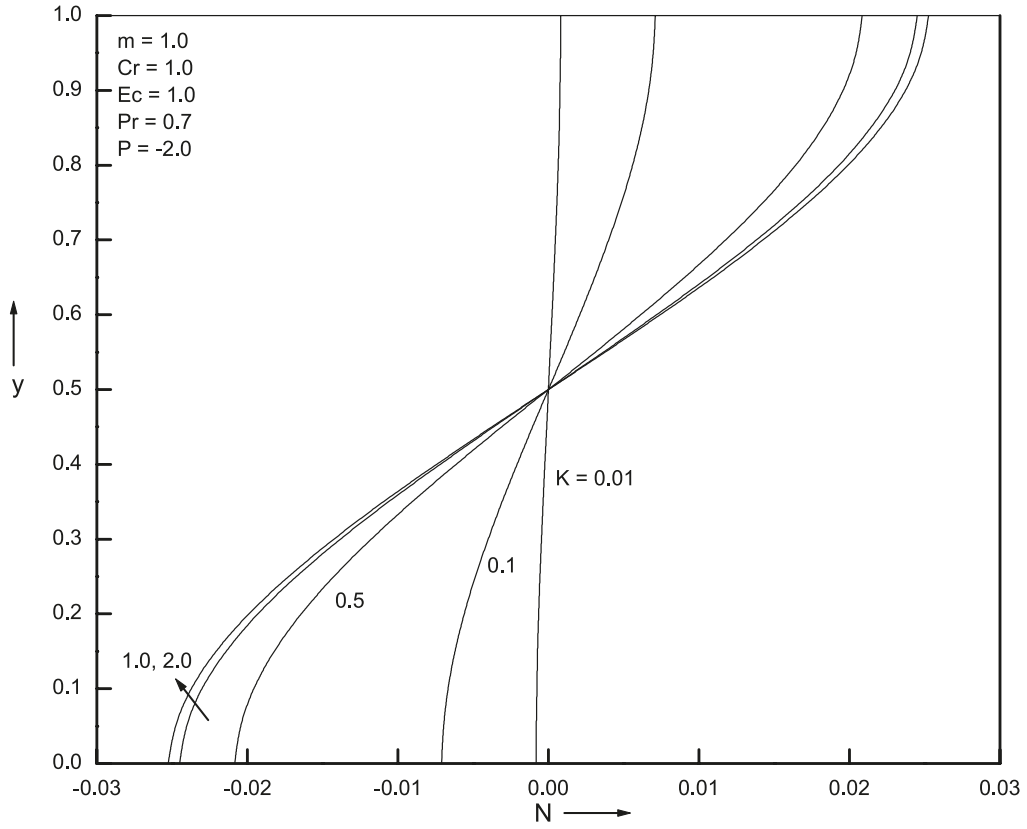

Fig. 10. Effects of the viscosity ratio m on the microrotation velocity profiles N.

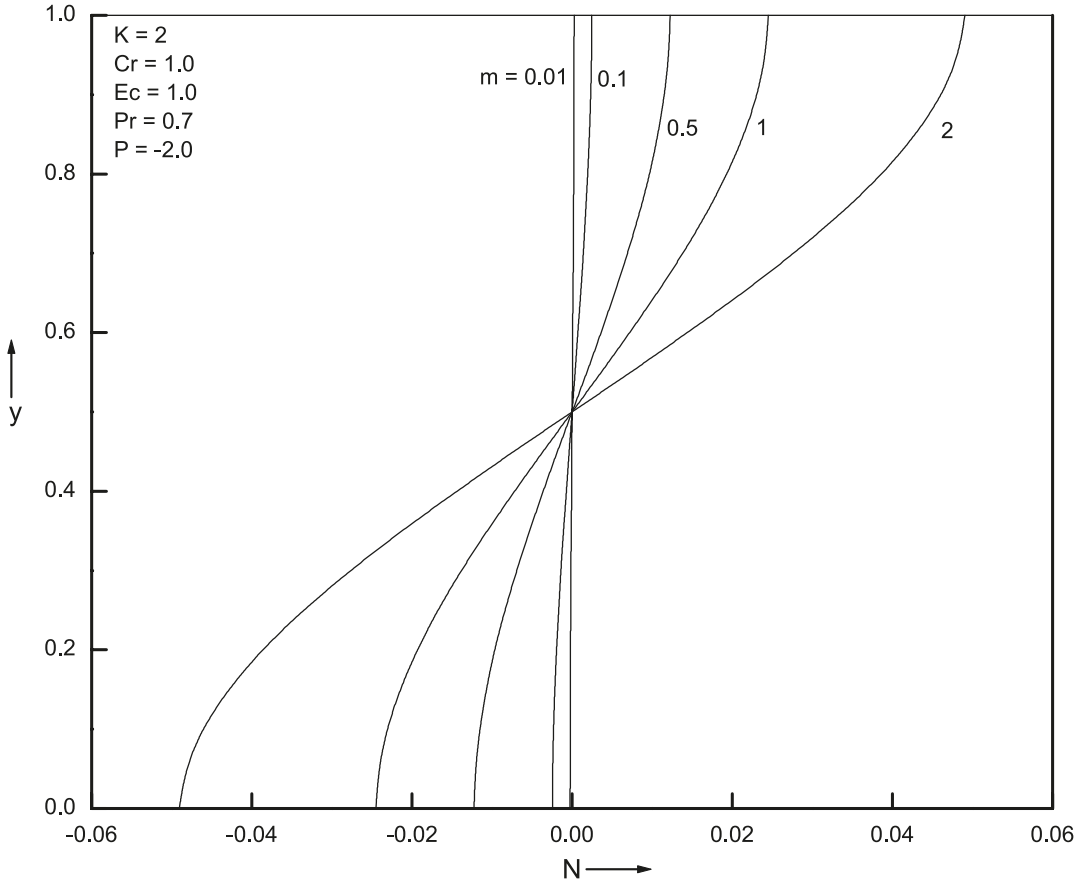

(Newtonian fluid) when compared with $K = 2$ (micropolar fluid).

Figure 4 displays the effect of the material parameter K on the temperature profiles. As K increases the temperature increases slightly in region-III and reverses its nature in the upper half of region-II. It is interesting to note that the temperature profile with K lies in between a Newtonian ($K = 0$) fluid in the presence and absence of viscous dissipation, respectively. Effects of the viscosity ratio m on the temperature profiles is shown in Fig. 5. As m increases the temperature profiles increases very slightly in region-III and decreases in region-I. Here also, the profiles with K lie in between a Newtonian ($K = 0$) fluid with and without viscous dissipation.

Figures 6 and 7 show the effect of Prandtl number Pr and Eckert number Ec on the temperature profiles. It is seen that as Pr and Ec increase the temperature profiles increases for both Newtonian ($K = 0$) and micropolar ($K \neq 0$) fluids. But the magnitude is large for the Newtonian fluid compared to the micropolar fluid, respectively. Figure 8 displays the effect of the conductivity ratio Cr on the temperature profiles. As the conductivity ratio increases, the temperature increases in the upper half of region-II and decreases in the lower half of region-II. It is very interesting to note that there is a common point for all values of the conductivity ratio exactly at $y = 0.5$ for both the Newtonian and micropolar fluids. Here, also temperature profiles are in between a Newtonian fluid with and without viscous dissipation.

Figures 9 and 10 illustrate the effect of the material parameter K and the viscosity ratio m on the microrotation velocity N. We notice that as K and m increase the microrotation velocity N decreases below $y = 0.5$ and increases above $y = 0.5$ and here also the profiles meet at a common point for all values of K and m.

Because of the importance of the viscosity suggested by Dintenfass [23], the shear viscosity μ of a micropolar fluid on the velocity and microrotation velocities for 20% and 40% RBC (Red blood corpuscles) concentration has been computed and is shown graphically in Figs. 11 and 12 for different values of K. In the present analysis the shear viscosity μ of the micropolar fluid is taken in the form μ_R/K where μ_R is cell rotational viscosity (the values of μ_R are taken from Ariman et al. [18]). For $K = 1$, the velocity increases as the concentration increases but decreases for $K = 2$. The present results can be obtained from Ariman et al. [18] replacing μ by μ_2 and μ_R by μK in cylindrical polar co-ordinates. Figure 12 shows the effect of the shear viscosity μ_R on the microrotation velocity N. We notice that N decreases as μ_R decreases (for both $K = 1, 2$) above $y = 0.5$ and the profiles are exactly reflected below $y = 0.5$.

The effect of the cell rotation μ_R for different solvent viscosities μ_1 on the flow velocity, microrotation velocity, and temperature profiles is shown in Tables 1–3, respectively. The effect is significant for large values of μ_1. The variation of rate of heat transfer, skin friction, and mass flow rate on various governing parameters such as viscosity ratio, conductivity ratio, material parameter, Eckert number, and Prandtl number is shown in Table 4.

Fig. 11. Variation of the effective viscosity μ on the velocity profiles.

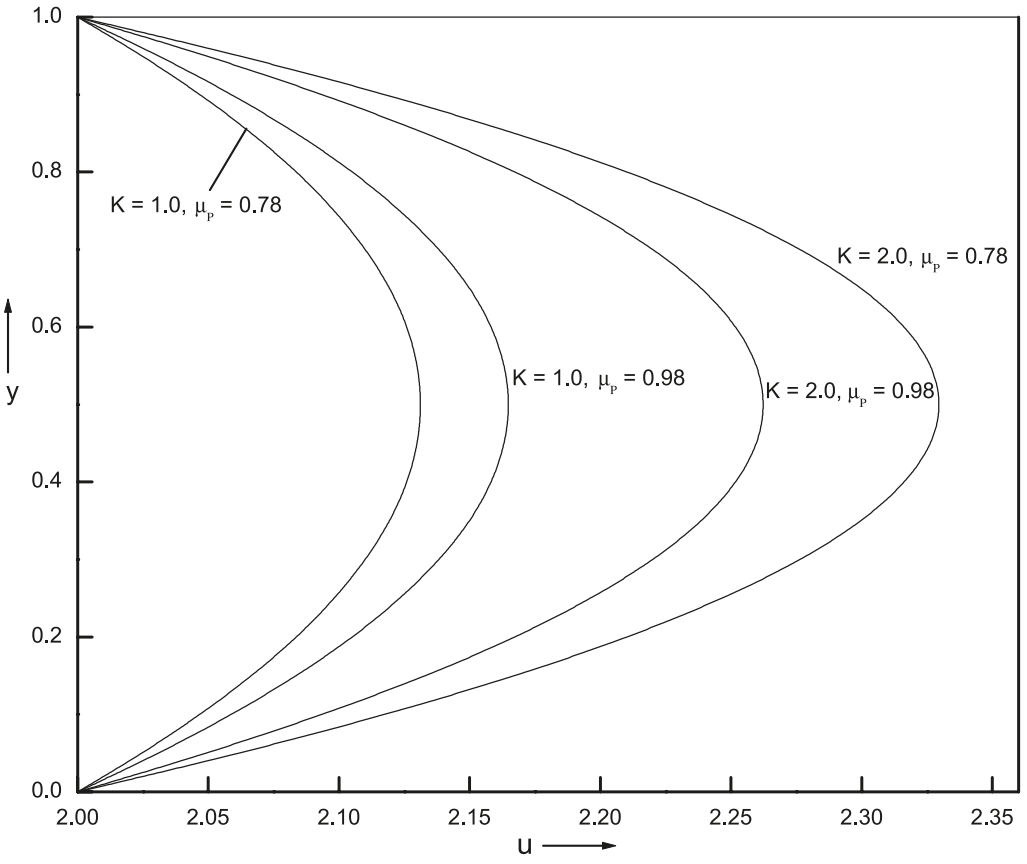

Table 1. The variation of cell rotational viscosity μ_R for different solvent viscosity μ_1 on velocity in region–II.

	$\mu_1 = 0.00018$ (Air)			$\mu_1 = 0.0114$ (Water)			$\mu_1 = 13.0$ (Glycerine)		
y	$\mu_R = 0.0$	$\mu_R = 0.78$	$\mu_R = 0.98$	$\mu_R = 0.0$	$\mu_R = 0.0$	$\mu_R = 0.78$	$\mu_R = 0.98$	$\mu_R = 0.0$	$\mu_R = 0.0$
1.00	2.00000	2.00000	2.00000	2.00000	2.00000	2.00000	2.00000	2.00000	2.00000
0.95	2.00000	2.00001	2.00000	2.00028	2.00036	2.00028	2.31692	2.4063	2.32339
0.90	2.00001	2.00001	2.00001	2.00053	2.00068	2.00054	2.6011	2.77064	2.61337
0.85	2.00001	2.00002	2.00001	2.00075	2.00096	2.00076	2.85234	3.09274	2.86973
0.80	2.00001	2.00002	2.00002	2.00094	2.0012	2.00096	3.07045	3.37237	3.09229
0.75	2.00002	2.00002	2.00002	2.0011	2.00141	2.00112	3.25527	3.60931	3.28088
0.70	2.00002	2.00002	2.00002	2.00123	2.00158	2.00126	3.40666	3.80341	3.43537
0.65	2.00002	2.00003	2.00002	2.00134	2.00171	2.00136	3.52453	3.95452	3.55564
0.60	2.00002	2.00003	2.00002	2.00141	2.00181	2.00144	3.60878	4.06254	3.64161
0.55	2.00002	2.00003	2.00002	2.00146	2.00187	2.00148	3.65935	4.12738	3.69322
0.50	2.00002	2.00003	2.00002	2.00147	2.00188	2.0015	3.67622	4.14899	3.71042
0.45	2.00002	2.00003	2.00002	2.00146	2.00187	2.00148	3.65935	4.12738	3.69322
0.40	2.00002	2.00003	2.00002	2.00141	2.00181	2.00144	3.60878	4.06254	3.64161
0.35	2.00002	2.00003	2.00002	2.00134	2.00171	2.00136	3.52453	3.95452	3.55564
0.30	2.00002	2.00002	2.00002	2.00123	2.00158	2.00126	3.40666	3.80341	3.43537
0.25	2.00002	2.00002	2.00002	2.0011	2.00141	2.00112	3.25527	3.60931	3.28088
0.20	2.00001	2.00002	2.00002	2.00094	2.0012	2.00096	3.07045	3.37237	3.09229
0.15	2.00001	2.00002	2.00001	2.00075	2.00096	2.00076	2.85234	3.09274	2.86973
0.10	2.00001	2.00001	2.00001	2.00053	2.00068	2.00054	2.6011	2.77064	2.61337
0.05	2.00000	2.00001	2.00000	2.00028	2.00036	2.00028	2.31692	2.4063	2.32338
0.00	2.00000	2.00000	2.00000	2.00000	2.00000	2.00000	2.00000	2.00000	2.00000

Fig. 12. Variation of the effective viscosity on the microrotation velocity profiles.

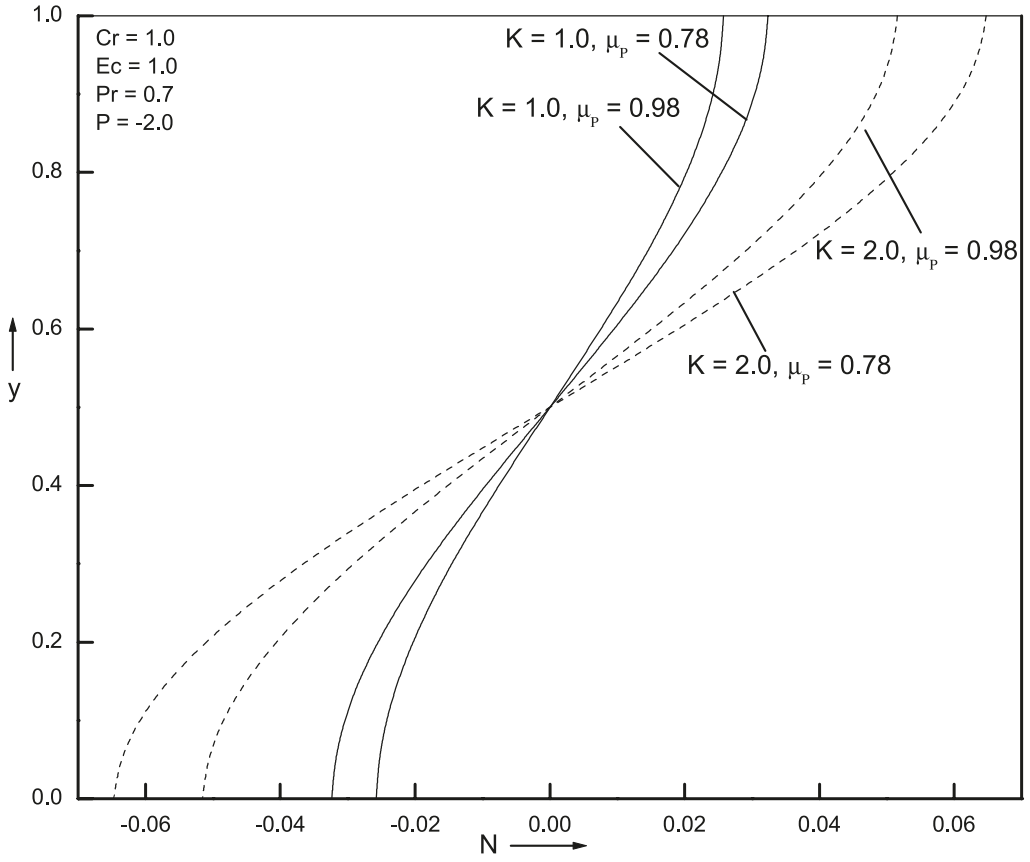

Table 2. The variation of cell rotational viscosity μ_R for different solvent viscosity μ_1 on microrotation velocity in region–II.

	$\mu_1 = 0.00018$ (Air)			$\mu_1 = 0.0114$ (Water)			$\mu_1 = 13.0$ (Glycerine)		
y	$\mu_R = 0.0$	$\mu_R = 0.78$	$\mu_R = 0.98$	$\mu_R = 0.0$	$\mu_R = 0.78$	$\mu_R = 0.98$	$\mu_R = 0.0$	$\mu_R = 0.78$	$\mu_R = 0.98$
1.00	0.00	0.00001	0.00	0.00029	0.00037	0.00029	0.32832	0.42092	0.33502
0.95	0.00	0.00001	0.00	0.00028	0.00036	0.00029	0.32349	0.41473	0.33009
0.90	0.00	0.00001	0.00	0.00027	0.00035	0.00028	0.30972	0.39708	0.31604
0.85	0.00	0.00001	0.00	0.00025	0.00032	0.00026	0.28806	0.3693	0.29394
0.80	0.00	0.00000	0.00	0.00023	0.00029	0.00023	0.25953	0.33273	0.26483
0.75	0.00	0.00000	0.00	0.0002	0.00025	0.00020	0.22515	0.28865	0.22974
0.70	0.00	0.00000	0.00	0.00016	0.00021	0.00017	0.18591	0.23835	0.18971
0.65	0.00	0.00000	0.00	0.00013	0.00016	0.00013	0.14281	0.18309	0.14572
0.60	0.00	0.00000	0.00	0.00008	0.00011	0.00009	0.09681	0.12411	0.09878
0.55	0.00	0.00000	0.00	0.00004	0.00005	0.00004	0.04888	0.06267	0.04988
0.50	0.00	0.00000	0.00	0.00000	0.00000	0.00000	0.00000	0.00000	0.00000
0.45	0.00	0.00000	0.00	−0.00004	−0.00005	−0.00004	−0.04889	−0.06267	−0.04988
0.40	0.00	0.00000	0.00	−0.00008	−0.00011	−0.00009	−0.09681	−0.12411	−0.09878
0.35	0.00	0.00000	0.00	−0.00013	−0.00016	−0.00013	−0.14281	−0.18309	−0.14572
0.30	0.00	0.00000	0.00	−0.00016	−0.00021	−0.00017	−0.18591	−0.23835	−0.18971
0.25	0.00	0.00000	0.00	−0.0002	−0.00025	−0.0002	−0.22515	−0.28865	−0.22974
0.20	0.00	0.00000	0.00	−0.00023	−0.00029	−0.00023	−0.25953	−0.33273	−0.26483
0.15	0.00	−0.00001	0.00	−0.00025	−0.00032	−0.00026	−0.28806	−0.3693	−0.29394
0.10	0.00	−0.00001	0.00	−0.00027	−0.00035	−0.00028	−0.30972	−0.39708	−0.31604
0.5	0.00	−0.00001	0.00	−0.00028	−0.00036	−0.00029	−0.32349	−0.41473	−0.33009
0.00	0.00	−0.00001	0.00	−0.00029	−0.00037	−0.00029	−0.32832	−0.42092	−0.33502

Table 3. The variation of cell rotational viscosity μ_R for different solvent viscosity μ_1 on temperature in region–II.

	$\mu_1 = 0.00018$ (Air)			$\mu_1 = 0.0114$ (Water)			$\mu_1 = 13.0$ (Glycerine)		
y	$\mu_R = 0.0$	$\mu_R = 0.78$	$\mu_R = 0.98$	$\mu_R = 0.0$	$\mu_R = 0.0$	$\mu_R = 0.78$	$\mu_R = 0.98$	$\mu_R = 0.0$	$\mu_R = 0.0$
1.00	1.44445	1.44445	1.44445	1.44454	1.44457	1.44454	1.55433	1.58533	1.55658
0.95	1.41417	1.41417	1.41417	1.41427	1.41429	1.41427	1.52675	1.55851	1.52905
0.90	1.38389	1.38389	1.38389	1.38399	1.38401	1.38399	1.49429	1.52544	1.49655
0.85	1.35361	1.35361	1.35361	1.35370	1.35373	1.35370	1.45797	1.48740	1.46010
0.80	1.32333	1.32334	1.32333	1.32342	1.32344	1.32342	1.41867	1.44556	1.42061
0.75	1.29306	1.29306	1.29306	1.29313	1.29315	1.29313	1.37717	1.40089	1.37889
0.70	1.26278	1.26278	1.26278	1.26284	1.26286	1.26284	1.33414	1.35427	1.33560
0.65	1.23250	1.23250	1.23250	1.23255	1.23256	1.23255	1.29013	1.30638	1.29130
0.60	1.20222	1.20222	1.20222	1.20226	1.20227	1.20226	1.24555	1.25777	1.24643
0.55	1.17194	1.17194	1.17194	1.17197	1.17198	1.17197	1.20072	1.20884	1.20131
0.50	1.14167	1.14167	1.14167	1.14168	1.14168	1.14168	1.15582	1.15981	1.15611
0.45	1.11139	1.11139	1.11139	1.11139	1.11139	1.11139	1.11091	1.11077	1.11090
0.40	1.08111	1.08111	1.08111	1.08110	1.08109	1.08110	1.06592	1.06164	1.06561
0.35	1.05083	1.05083	1.05083	1.05081	1.05080	1.05081	1.02068	1.01218	1.02007
0.30	1.02055	1.02055	1.02055	1.02052	1.02050	1.02051	0.97489	0.96200	0.97395
0.25	0.99028	0.99028	0.99028	0.99022	0.99021	0.99022	0.92810	0.91056	0.92683
0.20	0.96000	0.96000	0.96000	0.95993	0.95991	0.95993	0.87978	0.85716	0.87815
0.15	0.92972	0.92972	0.92972	0.92963	0.92961	0.92963	0.82927	0.80094	0.82722
0.10	0.89944	0.89944	0.89944	0.89934	0.89931	0.89933	0.77578	0.7409	0.77326
0.05	0.86916	0.86916	0.86916	0.86903	0.86900	0.86903	0.71843	0.67591	0.71535
0.00	0.83889	0.83889	0.83889	0.83873	0.83868	0.83873	0.65619	0.60467	0.65247

Table 4. The rate of heat transfer, the skin friction at the top and bottom plates, and the mass flow rate for different values of m, Cr, K, Ec, and Pr.

	m	q_T	q_B	τ_T	τ_B	MFR
m	0.01	−23.8945	3.28881	−3.0000	3. 0000	4.33392
	0.5	−23.8962	3.28513	−3.0000	3. 0000	4.36274
	1.0	−23.8980	3.28137	−3.0000	3. 0000	4.39215
	4.0	−23.9085	3.25883	−3.0000	3. 0000	4.56861
Cr	0.01	−23.5943	3.58506	−3.0000	3. 0000	4.39215
	0.5	−23.7746	3.40469	−3.0000	3. 0000	4.39215
	1.0	−23.898	3.28137	−3.0000	3. 0000	4.39215
	4.0	−24.2062	2.97308	−3.0000	3. 0000	4.39215
K	0.01	−23.9325	3.25058	−3.0000	3. 0000	4.49835
	0.5	−23.9103	3.26741	−3.0000	3. 0000	4.44583
	1.0	−23.9029	3.27484	−3.0000	3. 0000	4.41919
	4.0	−23.8956	3.28566	−3.0000	3. 0000	4.36973
Ec	0.01	0.09102	0.36281	−3.0000	3. 0000	4.39215
	0.5	−11.7823	1.80735	−3.0000	3. 0000	4.39215
	1.0	−23.898	3.28137	−3.0000	3. 0000	4.39215
	4.0	−96.5918	12.1255	−3.0000	3. 0000	4.39215
Pr	0.01	−0.01283	0.37545	−3.0000	3. 0000	4.39215
	0.5	−16.9747	2.43908	−3.0000	3. 0000	4.39215
	1.0	−34.2828	4.54482	−3.0000	3. 0000	4.39215
	4.0	−138.131	17.17928	−3.0000	3. 0000	4.39215

7. Conclusion

Both analytical and numerical solutions have been obtained for the steady flow in a horizontal channel consisting of a core region assumed to be a micropolar fluid and two viscous (Newtonian) fluid regions. The solutions are shown graphically for various governing parameters such as the material parameter, viscosity ratio, conductivity ratio, Eckert and Prandtl numbers on flow velocity, and microrotation and temperature profiles. In addition, results for the rate of heat transfer, mass flow rate,

and skin friction for different values of the physical parameters are presented in tabular form. It was found that the effect of the material parameter is to suppress the flow and the viscosity ratio promotes the flow. It is also interesting to note that the material parameter and viscosity ratio affect the position of the point of flow separation for which the flow nature is reversed. The analysis presented here indicates that a micropolar fluid model can yield results that differ from those obtained with a classical Newtonian formulation.

References

1. A.C. Eringen. J. Math. Mech. **16**, 1 (1966).
2. A.C. Eringen. J. Math. Analysis Appl. **38**, 480 (1972).
3. A.J. Willson. Proc. Camb. Philos. Soc. **67**, 469 (1970).
4. R.F. Bergholz. ASME J. Heat Trans. **102**, 242 (1980).
5. B. Chandra Shekar, P. Vasseur, L. Robillard, and T.H. Nguyen. Can. J. Chem. Eng. **62**, 482 (1984).
6. J. Peddieson and R.P. McNitt. Adv. Eng. Sci. **5**, 405 (1970).
7. T. Ariman, M.A. Truk, and N.D. Sylvester. Int. J. Eng. Sci. **11**, 905 (1973).
8. G. Łukaszewicz. Micropolar fluids: theory and application. Birkhäuser, Basel. 1999.
9. A.C. Eringen. Microcontinuum field theories. ii: fluent media. Springer, New York. 2001.
10. L.E. Bayliss. Rheology of blood and lymph, deformation and flow in biological systems. *Edited by* A. Fry-Wyssling. North-Holland Publishing Company, Amsterdam. 1952. p. 354.
11. Y.C. Fung. Fed. Proc. **25**, 1761 (1966).
12. H.S. Lew and Y.C. Fung. J. Biomech. **3**, 23 (1970).
13. R.L. Whitmore. Rheology of the circulation. Pergamon Press Oxford. 1968.
14. G. Bugliarello and J. Sevilla. Biorheology, **7**, 85 (1970).
15. H.L. Goldsmith and R. Skalak. Hemodynamics. Palo Alto Publ. 231. Annual Review Inc., Calif. 1975.
16. G.R. Cocklet and Y.C. Fung (*Editors*). The rheology of human blood. *In* Biomechanics: its foundation and objectives. Englewood Cliffs, Prentice-Hall Publicity. 1972.
17. G. Radhakrishnamacharya. Int. J. Eng. Sci. **15**, 719 (1977).
18. T. Ariman, M.A. Turk, and N.D. Sylvester. ASME J. Appl. Mech. **41**, 1 (1974).
19. H.R. Haynes. Am. J. Physiol. **198**, 1193 (1960).
20. G. Ahmadi. Int. J. Eng. Sci. **14**, 639 (1976).
21. D.A.S. Rees and A.P. Bassom. Int. J. Eng. Sci. **34**, 113 (1996).
22. D.A.S. Rees and I. Pop. IMA J. Appl. Math. **61**, 179 (1998).
23. S. Dintensfass. Cardiovas. Med. **2**, 337 (1977).
24. P. Chaturani and V.S. Upadhya. Bioreheology, **16**, 419 (1979).

Nomenclature

Cr	thermal conductivity ratio
Ec	Eckert number
h	height of each stratum (m)
j	microinertia density (m^2)
k_1	thermal conductivity of the fluids in regions–I and III ($W\,m^{-1}\,K^{-1}$)
k_2	thermal conductivity of the fluid in the region–II ($W\,m^{-1}\,K^{-1}$)
K	micropolar parameter
m	viscosity ratio
N	component of microrotation (s^{-1})
p	pressure ($kg\,m^{-1}\,s^{-2}$)
P	non-dimensional pressure
Pr	Prandtl number
q	non-dimensional rate of heat transfer
T_i	fluid temperature in the three regions (K)
T_{w1}	temperature of the upper plate (K)
T_{w2}	temperature of the lower plate (K)
u_i	x-component of fluid velocity in the three regions ($m\,s^{-1}$)
$\bar{u}_1$	average velocity ($m\,s^{-1}$)
x	coordinate in the axial direction (m)
y	coordinate in the transversal direction (m)

Greek symbols

γ	spin gradient viscosity ($kg\,m\,s^{-1}$)
κ	vortex viscosity ($kg\,m^{-1}\,s^{-1}$)
μ	viscosity of the micropolar fluid ($kg\,m^{-1}\,s^{-1}$)
μ_1	viscosity of the clear fluid ($kg\,m^{-1}\,s^{-1}$)
μ_R	cell rotational viscosity ($kg\,m^{-1}\,s^{-1}$)
θ_i	non-dimensional fluid temperature in the three regions
τ	skin friction coefficient

Superscript

*	non-dimensional variables defined in (7)

This article has been cited by:

1. J. C. Umavathi. 2011. Free convection of composite porous medium in a vertical channel. *Heat Transfer-Asian Research* **40**:4, 308-329. [CrossRef]